

Analysis of the Drag Angle in Cone Drum False Twisting Mechanism

Choon Gil Lee

Dept. of Textile and Fashion Technology, Kyungil University, Kyungsan, Korea

Abstract : The newly developed cone drum twister is one of the outer surface contacting friction-twisting devices in false-twist texturing. An investigation of the drag angle for the newly developed cone drum twister texturing mechanism is reported. An analysis is given from which equations can be derived that relate to the conical angle of cone drum, wrapping angle, drag angle, and yarn helix angle. Theoretical values of drag angle are calculated and discussed. It is shown that, as the helix angle and the projected wrapping angle increases, the drag angle also increases slowly until the helix angle of 40° but after the helix angle of 40° the drag angle increases rapidly. Furthermore the higher the projected wrapping angle and conical angle, the higher the drag angle of friction surface.

Key words : drag angle, cone drum twister, outer surface contacting friction-twisting device, conical angle, projected wrapping angle, forward velocity of filament yarn, circumferential velocity resulting from twisting of filament yarn

NOMENCLATURE

b Beginning point of false twist inserting
 c End point of false twist inserting
 D Velocity of friction surface (mm/sec)
 D_b Velocity of friction surface at point b (mm/sec)
 D_c Velocity of friction surface at point c (mm/sec)
 K Ratio of cone drum surface speed to forward yarn speed ($=D/V_1$)
 l Length of filament yarn in twisting zone, bc (mm)
 l_0 Length of bc in the flat drum (mm)
 p Any point on the line bc
 R Radius of the filament yarn (mm)
 r Cone drum radius at any point (mm)
 r_b Cone drum radius at point b (mm)
 r_c Cone drum radius at point c (mm)
 r_d Radius of the stud of cone drum (mm)
 s Length of bp (mm)
 V_0 Forward velocity of the zero twist filament yarn (mm/sec)
 V_1 Forward velocity of the twisted filament yarn in twisting zone (mm/sec)
 V_2 Circumferential velocity resulting from twisting of filament yarn in twisting zone (mm/sec)
 V_i Forward velocity of the filament yarn containing the twist angle, θ_i (mm/sec)
 V_R Surface velocity of the twisted filament yarn (mm/

sec)

α Angle between ob and op in the opening out diagram
 α_c Conical angle of cone drum
 α_o Angle between ob and oc in the opening out diagram
 β Angle between the yarn axis and the cone drum axis
 δ Angle between the drag velocity and the filament yarn axis
 ζ Drag velocity of the friction surface relative to the yarn surface
 θ Surface helix angle of the filament yarn in twisting zone
 λ Angle between ob and oo'
 ξ Angle of wrap (bp region) on the friction surface as seen perpendicular to the yz plane
 ξ^* Angle of wrap (bc region) on the friction surface as seen perpendicular to the yz plane
 ϕ Angle between the filament yarn axis and the direction of friction surface movement
 ω Angular velocity of cone drum (rad/sec)

INTRODUCTION

Mamy false twist methods have been used in synthetic fiber industry for the filament yarn texturing process. All kinds of conventional false twist methods have drive systems for inserting twist to the filament yarns. But the cone drum twister has no drive system for inserting false twist. A filament yarn passes over the surface of the cone

drum which rotates by the passing yarn without any special driving device.

The effects of various parameters on the false twisting tension and the yarn helix angle of the texturing yarns and physical properties of textured yarn produced by the cone drum twister were studied experimentally in previous studies (Lee & Kang, 1996). Also the effects of stud radius on dimensionless torque and the physical properties of the textured yarns in the stud type cone drum twister also had been studied (Lee, 1995). Also in addition the theoretical calculation of the relative velocity of friction surface of the system also had been studied (Lee, 2000).

The purpose of this paper is to develop theoretical relations between the cone drum geometry and the yarn geometry, and especially to calculate the drag angle of the system. The drag angle of the cone drum twister is used to calculate the tension and torque of the yarns used in this apparatus.

THEORETICAL ANALYSIS OF DRAG ANGLE

The side view of the cone drum twister is shown in Fig. 1. The photograph of the cone drum twister is shown in Fig. 2. This texturing machine has of a pair of feed rollers, a heater for setting deformed yarn, a pair of cone drum twisters which forces yarn to rotate, and a pair of take-up rollers. The false twist is inserted on the *bc* region by friction between the filament yarn and the rotating cone drum surface. Therefore the cone drum twister is one of the outer surface contacting friction-twisting devices in false-twist texturing. In this cone drum twister, a filament yarn passes over the surface of the cone drum

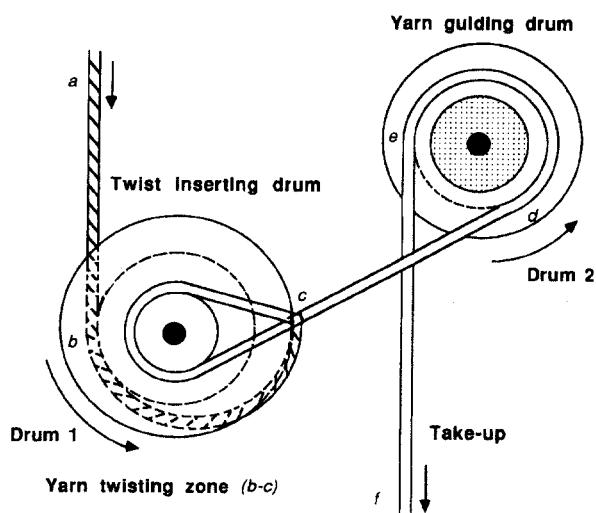


Fig. 1. Side view of the cone drum type draw texturing machine.

Fig. 2. Photograph of the cone drum type draw texturing machine.

which is rotated by the passing yarn wrapped the cone drum stud without a special driving device.

In order to analyze the drag angle in the false twisting mechanism theoretically, the false twisting contact region was considered. Our theoretical analysis of cone drum twister texturing process incorporates several simplifications and assumptions. The following assumptions were given in this analysis:

- (1) The filament yarn path remains straight in the open out diagram of the false twisting contact region, i.e., the yarn lies on the shortest path in the false twisting contact region.
- (2) The angle of the false twist in the false twisting contact region is constant.
- (3) The coefficient of friction is constant and independent of the cone drum shape and other variables.
- (4) The yarn is in continuous contact with the friction surface of the cone drum.
- (5) The normal forces between the filament yarn and the cone drum in the false twisting contact region are constant.
- (6) The yarn maintains a circular cross-section, radius R
- (7) Yarn bending moments, shear forces, and inertia forces are considered negligible in the false twisting contact region.

Drag velocity of the friction surface relative to the yarn surface

Fig. 3 shows the vector diagram at any point on the false twisting region of cone drum twister for the case of $D \cos \phi < V_1$. In this figure we can find the drag velocity of the friction relative to the filament yarn surface

The symbols used here are as follows:

V_1 : Forward velocity of the twisted filament yarn

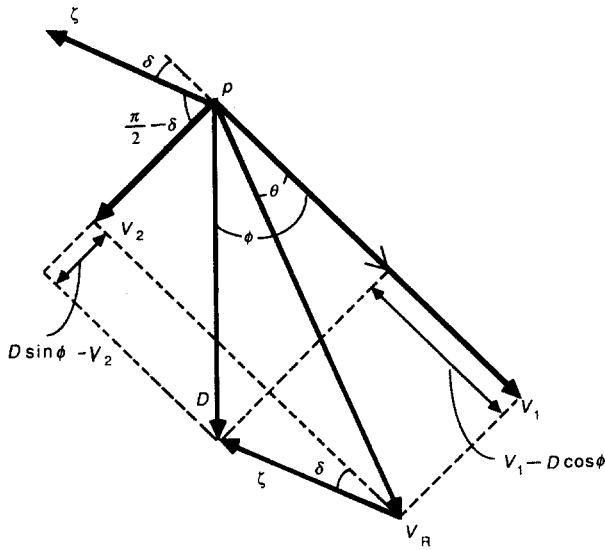


Fig. 3. Drag velocity of the friction surface relative to the yarn surface.

V_2 : Circumferential velocity of the filament yarn

V_R : Surface velocity of the filament yarn = $V_1 + V_2$

D : Velocity of friction surface

ζ : Drag velocity of the friction relative to the filament yarn surface

θ : Surface helix angle of the filament yarn, $\angle V_1 p V_R$

ϕ : Angle between the filament yarn axis and the velocity of friction surface

The relative velocity vector of D vector to V_R vector, ζ is the drag velocity of the friction relative to the filament yarn surface.

Angle between the drag velocity vector and the filament yarn axis, δ

Let the angle between drag velocity vector and filament yarn axis be δ . Then we get the following relation in Fig. 3.

$$\tan \delta = \frac{D \sin \phi - V_2}{V_1 - D \cos \phi} \quad (1)$$

Therefore the drag angle, δ is given by

$$\delta = \arctan \frac{D \sin \phi - V_R \sin \theta}{V_R \cos \theta - D \cos \phi} \quad (2)$$

and

$$\tan \theta = \frac{V_2}{V_1} \text{ so that } V = V_R \sin \theta \quad (3)$$

By inserting Equation (3) into Equation (1) we get

$$\tan \delta = \frac{K \sin \phi - \tan \theta}{1 - K \cos \phi} \quad (4)$$

where $K = D/V_1$ (Ratio of the speed of the cone drum

surface to the speed of yarn path)

Therefore

$$\delta = \arctan \frac{K \sin \phi - \tan \theta}{1 - K \cos \phi} \quad (5)$$

In Equation (1) $\delta = 0$ when $D \sin \phi - V_2 = 0$; In this case the total slippage occurs along the yarn path only. And $\delta = \pi/2$ when $V_1 - D \cos \phi = 0$; Hence in this case the total slippage is in the twisting direction only.

When $\phi < \pi/2$ then the output tension is higher than the input tension and vice versa.

Calculation of the angle between the filament yarn axis and the velocity of friction surface, ϕ

Calculation of the angle between the filament yarn axis and the velocity of friction surface at the beginning point of false twisting, λ

In Fig. 4, the angle between the filament yarn axis and the velocity of friction surface at any point p , ϕ is equal to $\angle poo'$ and the following relation is given;

$$\beta + \phi = \frac{\pi}{2} \quad (6)$$

where β is the angle between the filament yarn axis and the cone drum axis.

Therefore in this figure, if we let $\angle boo'$ be λ and β at point b be β_b , we obtain the following relation;

$$\lambda = \frac{\pi}{2} - \beta_b \quad (7)$$

The angle λ is equal to ϕ_b , which is the angle between the filament yarn axis and the velocity of friction surface at the beginning point of false twisting. The value of λ is obtained by using the relations between parameters in Fig. 4 and it is given that

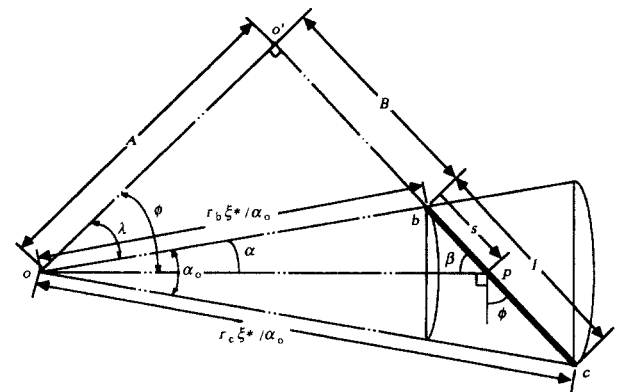


Fig. 4. Relationship between the cone drum radius at any point and the length between the beginning point b and any point p on the false twisting region.

$$\lambda = \cos^{-1} \frac{\left[\left(r_b \operatorname{cosec} \frac{\alpha_c}{2} \right)^2 - \frac{1}{4l^2} \left\{ \operatorname{cosec}^2 \frac{\alpha_c}{2} (r_c^2 - r_b^2) - l^2 \right\} \right]^{\frac{1}{2}}}{r_b \operatorname{cosec} \frac{\alpha_c}{2}} \quad (8)$$

Calculation of the angle between the yarn axis and the cone drum axis, β

In Fig. 4 we obtain

$$\cos(\alpha + \lambda) = \frac{\overline{oo'}}{op} \quad (9)$$

and

$$\cos(\alpha_o + \lambda) = \frac{\overline{oo'}}{oc} \quad (10)$$

From the above Equations we obtain

$$\frac{\overline{op}}{oc} = \frac{\overline{oc} \cos(\alpha_o + \lambda)}{\cos(\alpha + \lambda)} \quad (11)$$

On the other hand,

$$\alpha_o : \xi^* = \alpha : \xi \quad (12)$$

From the above proportional relation we obtain

$$\alpha = \frac{\alpha_o}{\xi^*} \xi = \frac{r_b}{ob} \xi = \frac{r_c}{oc} \xi \quad (13)$$

By using these Equations we can derive the following result;

$$\beta = \sin^{-1} \frac{\left[\left(r_b \operatorname{cosec} \frac{\alpha_c}{2} \right)^2 - \frac{1}{4l^2} \left\{ \operatorname{cosec}^2 \frac{\alpha_c}{2} (r_c^2 - r_b^2) - l^2 \right\} \right]^{\frac{1}{2}}}{r_c \operatorname{cosec} \frac{\alpha_c}{2} \cos \left(\xi^* \sin \frac{\alpha_c}{2} + \lambda \right)} \cos \left(\sin \frac{\alpha_c}{2} \xi + \lambda \right) \quad (14)$$

Relation between the contacting length and the projected wrapping angle

Let us derive the relation between the contacting length from point b to any point p on the bc , s and the projected wrapping angle on the yz plane, ζ .

In Fig. 4 we get the following relation;

$$\tan(\alpha + \lambda) = \frac{\overline{ob'} (= B) + s}{\overline{oo'} (= A)} \quad (15)$$

By inserting Equation (10) into the above Equation and by using the relations between parameters in Fig. 4 we obtain the following relationship:

$$s = \left[\left(r_b \operatorname{cosec} \frac{\alpha_c}{2} \right)^2 - \frac{1}{4l^2} \left\{ \operatorname{cosec}^2 \frac{\alpha_c}{2} (r_c^2 - r_b^2) - l^2 \right\} \right]^{\frac{1}{2}} \tan \left(\sin \frac{\alpha_c}{2} \xi + \lambda \right) - \frac{1}{2l} \left\{ \operatorname{cosec}^2 \frac{\alpha_c}{2} (r_c^2 - r_b^2) - l^2 \right\} \quad (16)$$

where λ is given in Equation (8).

RESULTS AND DISCUSSION

Plotting of the angle between the filament yarn axis and the velocity of friction surface at the beginning point of false twisting, λ .

The effect of the projected wrapping angle and conical angle on the angle between the filament yarn axis and the velocity of friction surface at the beginning point of false twisting can be obtained by using Equation (8). Fig. 5 shows the plots of the effect of projected wrapping angle and the conical angle on the angle between the filament yarn axis and the velocity of friction surface at the beginning point of false twisting: The higher the projected wrapping angle and conical angle the lower the angle between the filament yarn axis and the velocity of friction surface at the beginning point of false twisting.

Plotting of sine of the angle between the yarn axis and the cone drum axis, $\sin \beta$

By using Equation (14) we can plot the effect of the projected angle and the conical angle on $\sin \beta$ at the projected wrapping angle of 300° . Fig. 6 shows the relation between the projected angle and $\sin \beta$ at various conical angles. In this Figure, the higher the conical angle the

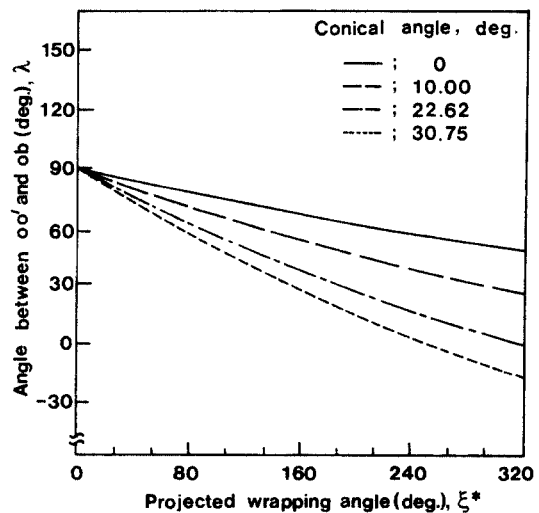


Fig. 5. Effect of projected wrapping angle and conical angle on the angle between the filament yarn axis and the velocity of friction surface at the beginning point of false twisting.

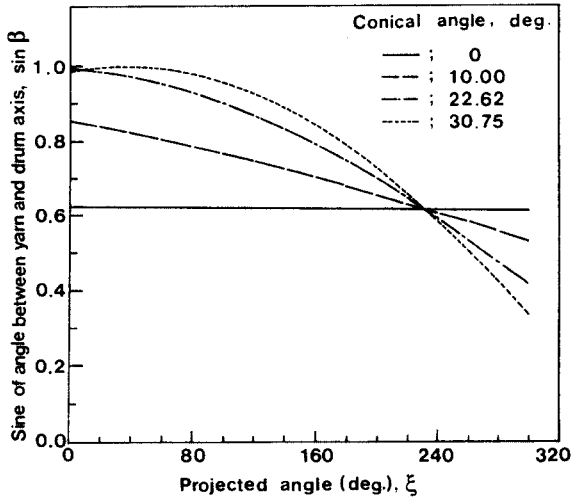


Fig. 6. Effect of projected angle and conical angle on $\sin \beta$ at the projected wrapping angle of 300° .

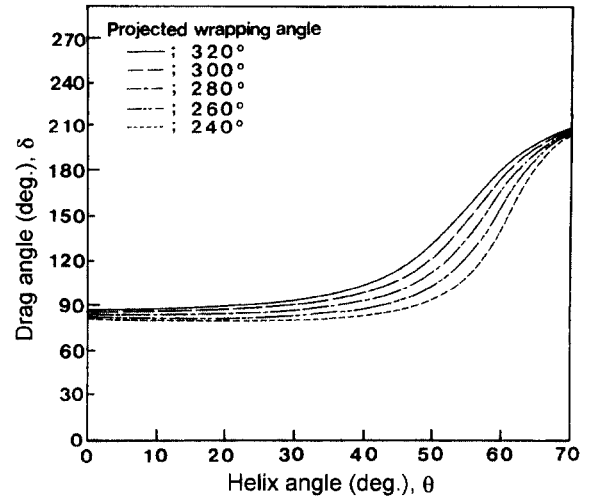


Fig. 8. Drag angle versus yarn helix angle at various projected wrapping angles under the conical angle of 0° .

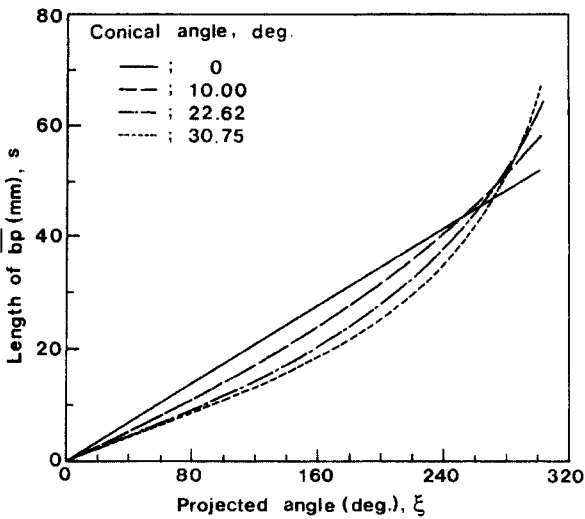


Fig. 7. Relation between the contacting length from point b to any point p on the bc, s and the projected wrapping angle on the yz plane at the projected wrapping angle of 300° .

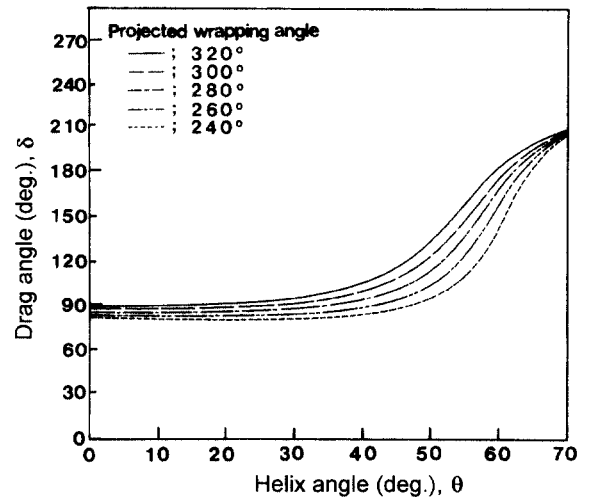


Fig. 9. Drag angle versus yarn helix angle at various projected wrapping angles under the conical angle of 10° .

higher $\sin \beta$ at low projected angle, but according to the increase of the projected angle, $\sin \beta$ decreased. The higher the conical angle the higher the decreasing rate of $\sin \beta$.

Relation between the contacting length and the projected wrapping angle at various conical angles

Fig. 7 shows the relation between the contacting length from point b to any point p on the bc, s and the projected wrapping angle on the yz plane, ζ by using Equation (16). Through this plot the following result is obtained: The higher the conical angle the lower the contacting length but the higher the increasing rate.

Effect of yarn helix angle, conical angle and projected wrapping angle on the drag angle of friction surface

After substituting Equations (8) and (16) into Equation (14), we obtain the value of drag angle by inserting this Equation into Equation (4). Figs. 8~11 show the plots of drag angle versus the yarn helix angle at various projected wrapping angles for the conical angles of 0, 10, 22.62, 30.75° respectively.

These plots show the effect of the yarn helix angle and the conical angle of the cone drum on the drag angle of the cone drum. These results will be affect the theoretical values of dimensionless torque and twisting efficiency. Through Figs. 8~11, we see that the drag angle of the friction surface increases slightly as the yarn helix angle

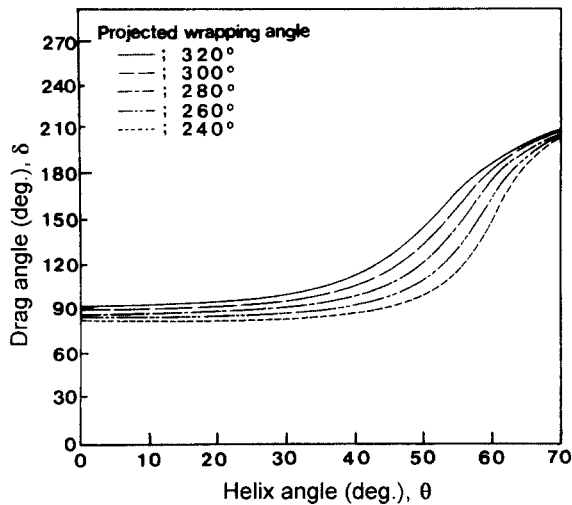


Fig. 10. Drag angle versus yarn helix angle at various projected wrapping angles under the conical angle of 22.62° .

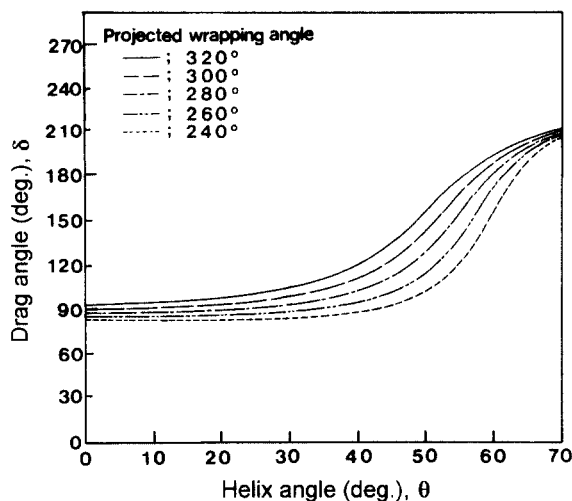


Fig. 11. Drag angle versus yarn helix angle at various projected wrapping angles under the conical angle of 30.75° .

increases until the yarn helix angle of 40° but beyond this angle the drag angle of the friction surface increases rapidly as the yarn helix angle increases. And these Figures show a similar increasing tendency for all projected wrapping angles but the higher the projected wrapping angle, the higher the drag angle of friction surface. Also the higher the conical angle the higher the drag angle of friction surface.

CONCLUSIONS

For the newly developed cone drum twister texturing mechanism, the analysis of the drag angle of friction surface is investigated theoretically. An analysis is given from which Equations can be derived that relate the con-

ical angle of the cone drum, the wrapping angle, the drag angle, and the yarn helix angle. Theoretical values of the drag angle were calculated and plotted.

Through the plotting of theoretical values of the drag angle of the friction surface, the following results were obtained.

1. The higher the projected wrapping angle and conical angle, the lower the angle between the filament yarn axis and the velocity of friction surface at the beginning point of false twisting.

2. The higher the conical angle, the higher $\sin \beta$ at low projected angle, but according to the increase of projected angle, $\sin \beta$ decreased. The higher the conical angle the higher the decreasing rate of $\sin \beta$.

3. The higher the conical angle the lower the contacting length but the higher the increasing rate.

4. The drag angle of the friction surface increases slightly as the yarn helix angle increases until a yarn helix angle of 40° , but over this angle the drag angle of the friction surface increases rapidly as the yarn helix angle increases.

5. The higher the projected wrapping angle and conical angle, the higher the drag angle of friction surface.

REFERENCES

- Lee C.G. (2000) Analysis of the relative velocity of friction surface in cone drum false twisting mechanism. *Journal of Korean Society for clothing Industry*, **2**(5), 443-449.
- Lee C.G. and Kang T.J. (1996) False twist tension and false twist angle in the cone drum twister. *Journal of Korean Fiber Society*, **33**(3), 248-256.
- Lee C.G. and Kang T.J. (1996) On the physical properties of textured yarn produced by the cone drum twister. *Journal of Korean Fiber Society*, **33**(5), 393-402.
- Lee C.G. (1995) Studies on the development of a stud type cone drum twister (I). *Journal of Korean Fiber Society*, **32**(7), 621-634.
- Kang T.J. (1988) Mechanics of high speed texturing, Part II: Theoretical analysis of ring twisting. *Text. Res. J.*, **58**(11), 653-662.
- Thwaites J.J. (1985) The mechanics of friction-twisting reassessed, Part II : Tension and torque generation in the disc spindle. *J. Textile Inst.*, **3**, 157-170.
- Thwaites J.J. (1978) The dynamics of the false-twist process, Part II: A theoretical model. *J. Textile Inst.*, **69**(9), 276-286.
- Morris W.J. and Denton M.J. (1975) An improved method of friction twisting in the false-twist-texturing process, Part II: theoretical relations between yarn and processing parameters in the improved friction spindle. *J. Textile Inst.*, **66**(3), 123-128.
- Howell H.G. (1953) The general case of friction of a string round a cylinder. *J. Textile Inst.*, T359-362.
- Theaites J.J. (1984) The mechanics of friction-twisting reassessed, Part I : The yarn path in a disc spindle. *J. Textile Inst.*, **75**(4), 285-297.
- Denton M.J. (1975) The structural geometry and mechanics of false-textured yarns. *J. Textile Inst.*, **66**(2), 80-86.

(Received September 28, 2001)